EFFECT OF THREE DIFFERENT BOUNDARY-LAYER PARAMETERISATIONS IN A REGIONAL ATMOSPHERIC MODEL ON THE SIMULATION OF SUMMER MONSOON CIRCULATION

K. V. J. POTTY and U. C. MOHANTY
Centre for Atmospheric Sciences, Indian Institute of Technology, New Delhi 110 016, India

S. RAMAN
Department of Marine, Earth and Atmospheric Sciences, North Carolina State University, Raleigh, NC 27695-8208, U.S.A.

(Received in final form 21 February, 1997)

Abstract. Bulk, first-order and turbulent kinetic energy (TKE) closure schemes are used to parameterise the boundary-layer physics in a high resolution, limited area model. The model was used to simulate the summer monsoon circulations over India. The domain selected included the monsoon trough over northern India, a region of mesoscale convection. A monsoon depression was present at the time of the simulation. The results indicate that the TKE closure scheme combined with the Monin–Obukhov surface-layer similarity relation provided the best 48-hour simulation of the circulation and the rainfall associated with the monsoon depression.

Key words: Indian summer monsoon circulation, Monsoon depression, Planetary boundary layer, Bulk method, First order closure scheme, TKE closure scheme

1. Introduction

The planetary boundary layer (PBL) plays an important role in numerical weather prediction (NWP) on different time scales (short, medium and extended ranges). The tropics act as a major source of heat and moisture and a sink of momentum for the global atmosphere, and these fluxes take place through the PBL. Therefore the inclusion of the PBL in NWP models over the tropics is very essential.

The parameterisation of the PBL in a NWP model consists of the computation of surface fluxes and the vertical distribution of these surface fluxes to the various model levels in the boundary layer. The computation and distribution of fluxes can be achieved in many ways depending upon the number of model levels (Clark, 1970; Deardorff, 1972) and the computer resources available. If the model has sufficient computational levels within the PBL, the distribution of the fluxes will be more realistic. Similarly, if a detailed physics is being employed for resolving the turbulent fluxes, a more realistic distribution can be achieved.

Sensitivity to the type of PBL parameterisation scheme in numerical models has been studied extensively by earlier researchers for different synoptic situations. For example, Mahfouf et al. (1987) compared the results of different PBL schemes against the Wangara data. They also compared the results of sea breeze flows over south Florida using a three dimensional model. The results show that the simulation with a TKE scheme is more realistic. Holt et al. (1990) studied the effects of

Boundary-Layer Meteorology **84:** 363–381, 1997.

different parameterisations of the boundary layer in a three-dimensional, limited area weather forecast model using the observations from the Genesis of Atlantic Lows Experiment (GALE) and the results show that the TKE parameterisation provides better short term forecasts. Huang et al. (1989) showed that a model with TKE closure simulated mesoscale dynamics associated with topography in a much realistic way. However very few numerical sensitivity studies have been carried out over the Indian monsoon region. The aim of this paper is to investigate the effects of the differences in the boundary-layer parameterisation on short range weather prediction for the case of a monsoon depression. For this purpose, three different PBL parameterisation schemes are incorporated in a high-resolution, limited area weather forecast model. The numerical simulation results are evaluated for the Indian monsoon region and compared with each other and with the observations.

2. Numerical Experiments

For the first experimental setup (designated as **BLK**), the surface layer (constant flux layer) is parameterised by the bulk aerodynamic method. The surface-layer height is taken as the height of the first model level just above the surface. For the present study it is the 0.997 σ-level. Surface stresses in the east-west and the north-south directions are given by

$$\tau_x = \rho u_*^2 \frac{u}{|V|}, \tag{1}$$

$$\tau_y = \rho u_*^2 \frac{v}{|V|}, \tag{2}$$

where $|V|$ is the wind speed, ρ is air density and the friction velocity, u_*, is given by

$$u_* = \sqrt{C_D |V|^2}. \tag{3}$$

The drag coefficient (C_D) has been assumed to be 2.5×10^{-3} and 1.5×10^{-3} over land and over ocean respectively.

Surface fluxes of heat and moisture respectively are represented by

$$\overline{w'\theta'} = -u_* 0_*, \tag{4}$$

$$\overline{w'q'} = -u_* q_*, \tag{5}$$

where scaling parameters of temperature (θ_*) and moisture (q_*) are given as

$$\theta_* = C_E |V| \frac{\theta_{kk} - \theta_s}{u_*}, \tag{6}$$

$$q_* = C_E|V|\frac{q_{kk} - q_s}{u_*}. \tag{7}$$

The subscripts s and kk represent the near surface value and the model level just above the surface respectively. C_E is the bulk exchange coefficient for both heat and moisture.

Above the surface layer, the mixed layer is parameterised using the mixing length parameterisation of D'Jolov (1974). In this first-order closure scheme, the exchange coefficient (K_m) is computed as

$$K_m = l^2 S, \tag{8}$$

where

$$l = \frac{kz}{(\phi_m + kz/\lambda)}$$

and

$$S = \left[\left(\frac{\partial u}{\partial z}\right)^2 + \left(\frac{\partial v}{\partial z}\right)^2\right]^{1/2}.$$

Here λ = 2.7 $\times$ 10^{-4} $|G|/f$, k = 0.4 and ϕ_m is computed by the Businger–Dyer relationship (Dyer, 1974), G is the geostrophic wind and f is the Coriolis parameter.

In the second experimental setup (called **MOK**), the surface boundary layer is parameterised based on similarity theory (Monin and Yaglom, 1971)

$$\frac{\partial u}{\partial z} = \frac{u_*}{kz}\phi_m(z/L), \tag{9}$$

$$\frac{\partial \theta}{\partial z} = \frac{\theta_*}{kz}\phi_h(z/L), \tag{10}$$

$$\frac{\partial q}{\partial z} = \frac{q_*}{kz}\phi_h(z/L), \tag{11}$$

where ϕ_m and ϕ_h are the non-dimensional universal functions of the stability parameter z/L (Businger et al., 1971). The roughness length z_0 (m) is considered as a function of terrain height over land and is calculated from the equation (Krishnamurti et al., 1990)

$$z_0 = 0.15 + 0.2(236.8 + 18.42\,h)^2 \times 10^{-8}, \tag{12}$$

where h denotes the topographic height in metres. Over the ocean z_0 has been computed using Charnock's relation (1955),

$$z_0 = 0.015\,u_*^2/g. \tag{13}$$

For the computation of latent heat flux over land, ground wetness factor has to be specified or computed. For the present study, it has been provided as a function of albedo and is given as (Kumar, 1989)

$$\beta = 0.85(1.0 - \exp(-200.0(0.31 - \text{Albedo})^2)). \tag{14}$$

Here the mixed layer is parameterised as in the case of first experimental setup (D'jolov, 1974).

In the third and last experimental setup (noted as **TKE**), the surface layer is parameterised using Monin–Obukhov similarity theory as given in the second experiment. Above the surface layer, the PBL parameterisation uses the turbulent kinetic energy (TKE) $E - \epsilon$ closure with the constants of Detering and Etling (1985).

The prognostic equation for TKE (E) is given as

$$\frac{\partial E}{\partial t} = -\overline{u'w'}\frac{\partial u}{\partial z} - \overline{v'w'}\frac{\partial v}{\partial z} + \frac{g}{\theta}\overline{w'\theta'} - \frac{\partial}{\partial z}(\overline{w'E'} + \overline{p'w'}/\rho) - \epsilon. \tag{15}$$

The first two terms on the right hand side of the equation represent shear production, the third represents buoyancy production, the fourth turbulent transport and fifth is the dissipation of TKE.

The parameterisations of individual terms are given by Holt and Raman (1988) and not explained here. However the final form of the prognostic equation for turbulent kinetic energy is given as,

$$\begin{aligned}\frac{\partial E}{\partial t} &= K_m\left[\left(\frac{\partial u}{\partial z}\right)^2 + \left(\frac{\partial v}{\partial z}\right)^2\right] + \frac{g}{\theta}K_h\frac{\partial \theta}{\partial z} \\ &\quad + C_1\frac{\partial}{\partial z}\left(K_m\frac{\partial E}{\partial z}\right) - \epsilon.\end{aligned} \tag{16}$$

In a similar manner a prognostic equation for the dissipation of TKE is given as,

$$\begin{aligned}\frac{\partial \epsilon}{\partial t} &= C_3\frac{\epsilon}{E}\left(-\overline{u'w'}\frac{\partial u}{\partial z} - \overline{v'w'}\frac{\partial v}{\partial z} + \frac{g}{\theta}\overline{w'\theta'}\right) \\ &\quad - C_4\frac{\epsilon^2}{E} + C_5\frac{\partial}{\partial z}\left(K_m\frac{\partial \epsilon}{\partial z}\right),\end{aligned} \tag{17}$$

and its parameterised form is given as,

$$\begin{aligned}\frac{\partial \epsilon}{\partial t} &= C_3\frac{\epsilon}{E}\left[K_m\left[\left(\frac{\partial u}{\partial z}\right)^2 + \left(\frac{\partial v}{\partial z}\right)^2\right] - \frac{g}{\theta}K_h\frac{\partial \theta}{\partial z}\right] \\ &\quad - C_4\frac{\epsilon^2}{E} + C_5\frac{\partial}{\partial z}\left[K_m\frac{\partial \epsilon}{\partial z}\right].\end{aligned} \tag{18}$$

The relationship of eddy viscosity (K_m) and TKE in terms of dissipation is given by (Daly and Harlow, 1970)

$$K_m = C_2 E^2/\epsilon. \tag{19}$$

Holt and Raman (1988) studied the suitability of the values of constants used in the above equations of TKE and dissipation and found that constants of Detering and Etling (1985) work well. Hence for the present study, same set of constants have been used and are given as:

$$C_1 = 1.35, \quad C_2 = 0.026, \quad C_3 = 1.13, \quad C_4 = 1.9 \text{ and } C_5 = 0.77.$$

Solution of the turbulent kinetic energy equation requires the specification of E in the surface layer (Mailhot and Benoit, 1982), which should be a function of u_*, w_* and z/L. Based on Deardorff (1974) and Wyngaard (1975),

$$\begin{aligned} E &= 3.75\, u_*^2 \qquad z/L > 0 \\ E &= 3.75\, u_*^2 + 0.2 w_*^2 + (-z/L)^{2/3} u_*^2 \qquad z/L < 0 \\ \epsilon &= u_*^3/kz, \end{aligned} \tag{20}$$

where u_* is the friction velocity and w_* is convective velocity, which is given by

$$w_* = [(g/T) h (\overline{w' T_v'})_0]^{1/3}, \tag{21}$$

where the subscript zero denotes near-surface values and virtual temperature (T_v) flux is computed as:

$$\overline{w' T_v'} = \overline{w' T'} + 0.61 (T \overline{w' q'} + q \overline{w' T'}). \tag{22}$$

Here g is the acceleration due to gravity and h is the boundary-layer height, which is computed from the TKE of the previous iteration. h is given as the model level height at which TKE reduces to 0.05 m^2 s^{-2} or less. The upper boundary condition is taken as $E = \epsilon = 0$.

Over water bodies, the surface temperature can be considered to be constant as a boundary condition during a short range forecast. However, the land surface temperature may vary considerably over a period of 12 to 24 hours and hence its variation has to be computed for the lower boundary condition. Here the ground temperature has been computed using a energy balance equation following Lazic and Talenta (1990). Mean climatological sea surface temperature (SST) for the month of August is being used for oceanic points.

3. Model Description

A high resolution (0.5° longitude/latitude) hydrostatic primitive equation model with a terrain following coordinate system is used. The horizontal domain of the

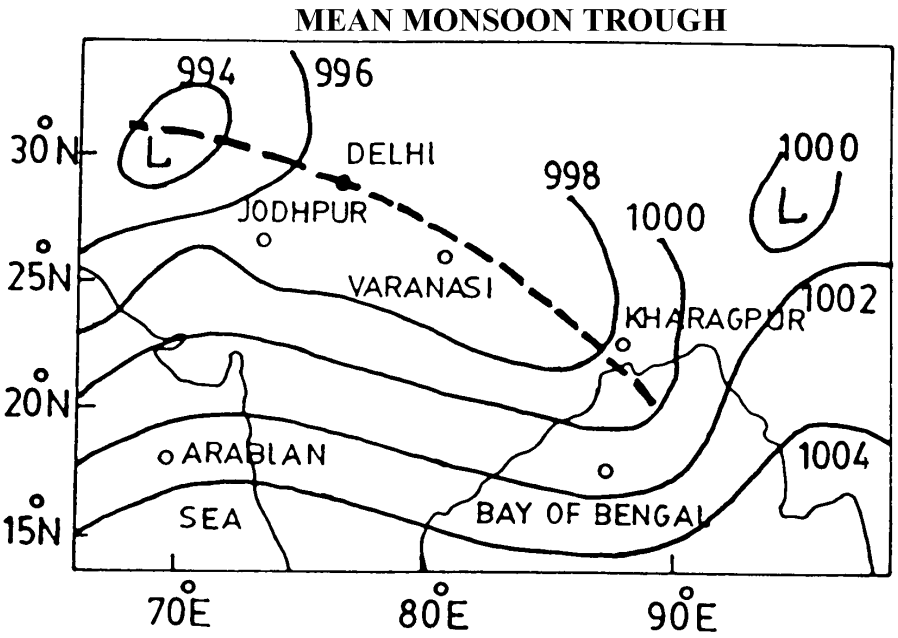

Figure 1. Model domain and grid points chosen for the study. (Source: India Meteorological Department.)

model is from 13.5° N to 34.5° N in the North–South direction and 66° E to 99° E in the east–west direction. The model domain of integration is given in Figure 1. On this figure the mean sea level pressure is presented to depict summer monsoon surface features and specific locations which are considered in the results are also marked. In the vertical, the model uses 16 levels (7 levels in the PBL) in sigma coordinates. The model uses an envelope topography based on the US Navy high resolution topographic data set. Details of the model equations and numerics may be obtained from Madala et al. (1987).

The seven governing equations (u and v momentum, temperature, moisture, surface pressure tendency, hydrostatic pressure and mass continuity) are given in surface pressure weighted flux form written for curvilinear horizontal coordinates. The terrain following variable (σ), defined as the ratio of pressure P to surface pressure P_s (Phillips, 1957) is chosen as the vertical coordinate.

The finite difference form of the governing equations is of second order accuracy in space. A split-explicit scheme (Madala, 1978) is used for time integration. The details of the time integration scheme employed in the model has been given by Mohanty et al. (1990). The C grid (Arakawa and Lamb, 1977) in the model has uniform resolution in longitude and latitude. On this grid, temperature (T), geopotential (ϕ), humidity (q) and $\dot{\sigma}$ are computed at mass points. The zonal component of the wind (u) is computed at the mid points along the X-axis and

meridional component (v) at mid points along the Y-axis; $\dot{\sigma}$ is evaluated at half σ levels.

A sponge boundary condition of Perkey and Kreitzberg (1976) is employed for updating the lateral boundaries of the model and a second order diffusion equation is used in the model to suppress the computational instabilities which arises due to the sub-grid scale processes.

The physical processes included in the model are dry convective adjustment, large-scale precipitation, convective precipitation and PBL mixing. Deep cumulus convection is parameterised based on the scheme of Kuo (Anthes, 1977). Convective precipitation occurs when low level moisture convergence exists in the convectively unstable environment. The distribution of latent heating and moisture is determined by the column mean relative humidity. The vertical distribution of the heating is considered to be proportional to the temperature difference between the pseudo adiabat and the environment.

Large-scale precipitation (Non-convective) occurs when saturation is reached on the grid scale. The Clausius–Clapyron equation is used to compute the excess moisture and the isobaric heating depending on the height where saturation occurs, a part of the excess moistening is assumed to precipitate into lower model layers and to re-evaporate. The remainder of the excess moisture precipitates to the surface. Dry convective adjustment is used when the static energy of the layer exceeds that of the adjacent higher layer. The adjustment results in slightly stable lapse rate, while the total static energy is conserved.

4. Data Sets for the Experiments

Numerical experiments have been performed to find out the most appropriate scheme for PBL parameterisation over the Indian region for simulation of monsoon circulations. The European Centre for Medium Range Weather Forecasts (ECMWF), U.K. operational analysis for 3 August 1988 at 1200 UTC has been used as initial conditions for integrating the model. US Navy topography data and climatological SST for the month of August have also been used for the model simulation.

5. Results and Discussion

Though the performance of a boundary-layer parameterisation scheme in an NWP model is ultimately evaluated by analyzing the simulation results of large scale fields, it is equally important to analyse the performance at individual grid points of the model as the summation of these grid point results represents the final output of the model. So it is helpful to analyse the simulation of different meteorological parameters at different grid points (or locations) before studying the large scale

fields. Since our aim in this paper is to compare the results produced by different PBL schemes and most of the PBL characteristics are diurnal in nature, it is mainly the 24 hour forecast that is used for the study even though the model has been integrated for 48 hours.

5.1. RESULTS AT SELECTED GRID POINTS

Eddy viscosity (K_m) in the PBL parameterisation determines the transport of heat, moisture and momentum in the PBL and the correction terms for wind, temperature and humidity of the model forecast. In Figure 2, the vertical profiles of K_m simulated by the three different PBL parameterisation schemes at 6 hour intervals are shown. In order to study characteristics over land and the oceans, one grid point has been selected over a land region (near Kharagpur) and one over the Arabian Sea (70° E, 19° N). Results show that there is a remarkable difference in the magnitude of K_m over the land and oceanic points, especially during day time. Distinct diurnal variation of K_m over land points can also be noticed in the figure. But these diurnal variations are not so pronounced over the oceanic region. Under solar insolation, land gets heated up much quicker than water bodies because of its lesser specific heat capacity. Turbulence transfer increases at a much faster rate with more intensity over land points due to the enhanced sensible heat flux. As eddy viscosity is a measure of turbulence, its magnitude is higher over land (5–13 $m^2\ s^{-1}$). During strong wind conditions, even at oceanic points, the maximum magnitude that K_m can reach is up to 25 $m^2\ s^{-1}$ owing to the large vertical shear (Holt and Raman, 1988). It is of interest to compare the simulation of K_m by different PBL parameterisation schemes at Kharagpur. The magnitude of the eddy viscosity computed by the Bulk method is least (7.1 $m^2\ s^{-1}$) and that simulated by the TKE scheme is the highest (12.8 $m^2\ s^{-1}$) at 11.30 LST. Since the vertical resolution of the model is somewhat coarse at about 200 m, all the three schemes computed maximum eddy viscosity at the same model level. Normally maximum K_m is at one third of the height of the boundary layer. In all the simulations, maximum K_m is at 220 m or at about one third the boundary-layer height of about 650 m (Figure 2). Again, in all the three cases, K_m decreases significantly above 600 m indicating the height of the boundary layer. Kusuma et al. (1991) estimated the boundary-layer height over the monsoon trough region during active and break phases and found that the boundary-layer height at Calcutta, a location close to Kharagpur is about 500 m during the active phase. They computed boundary-layer top as the height of the base of the capping inversion from virtual potential temperature profiles. Figure 3 shows the vertical profiles of virtual potential temperature (θ_v) as simulated by the three boundary-layer parameterisation schemes at 1200 UTC on Aug 4, 1988 (24 hr forecast) and the corresponding verification analysis at two land and oceanic grid points. It is clear that over Jodhpur and Kharagpur, the θ_v profile is more closely predicted by the TKE model. At Jodhpur, an inversion starts at about 1000 m as given by

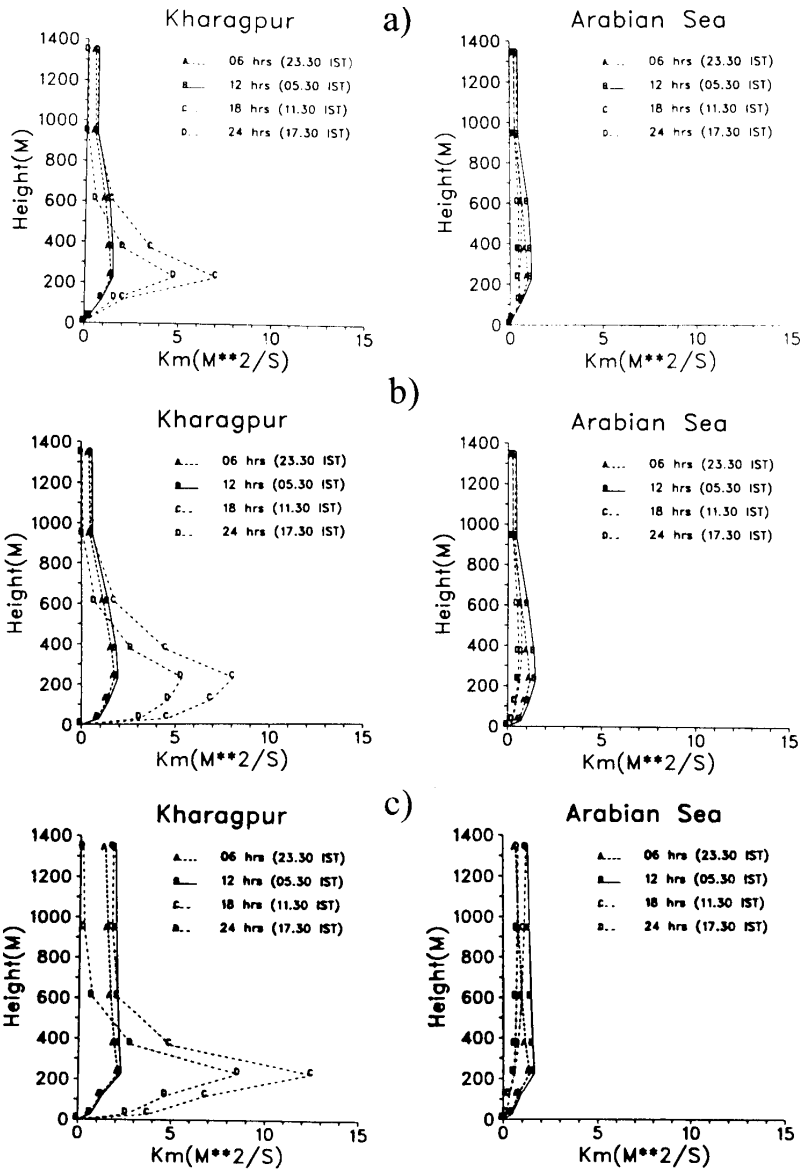

Figure 2. Vertical profiles of eddy viscosity at 6 hour intervals as simulated by the three different PBL parameterisation schemes (a) bulk method (b) first-order closure scheme and (c) TKE closure scheme.

the analysis and the TKE scheme whereas it starts at about 500 m for BLK and MOK. The virtual temperature is warmer for BLK and MOK below 1600 m at Kharagpur as compared with the TKE scheme (Figure 3b). It may be due to the fact that D'Jolov scheme does not see the inversion layer above the PBL as shown by Holt and Raman (1988). Except at the lower levels, both the first-order closure

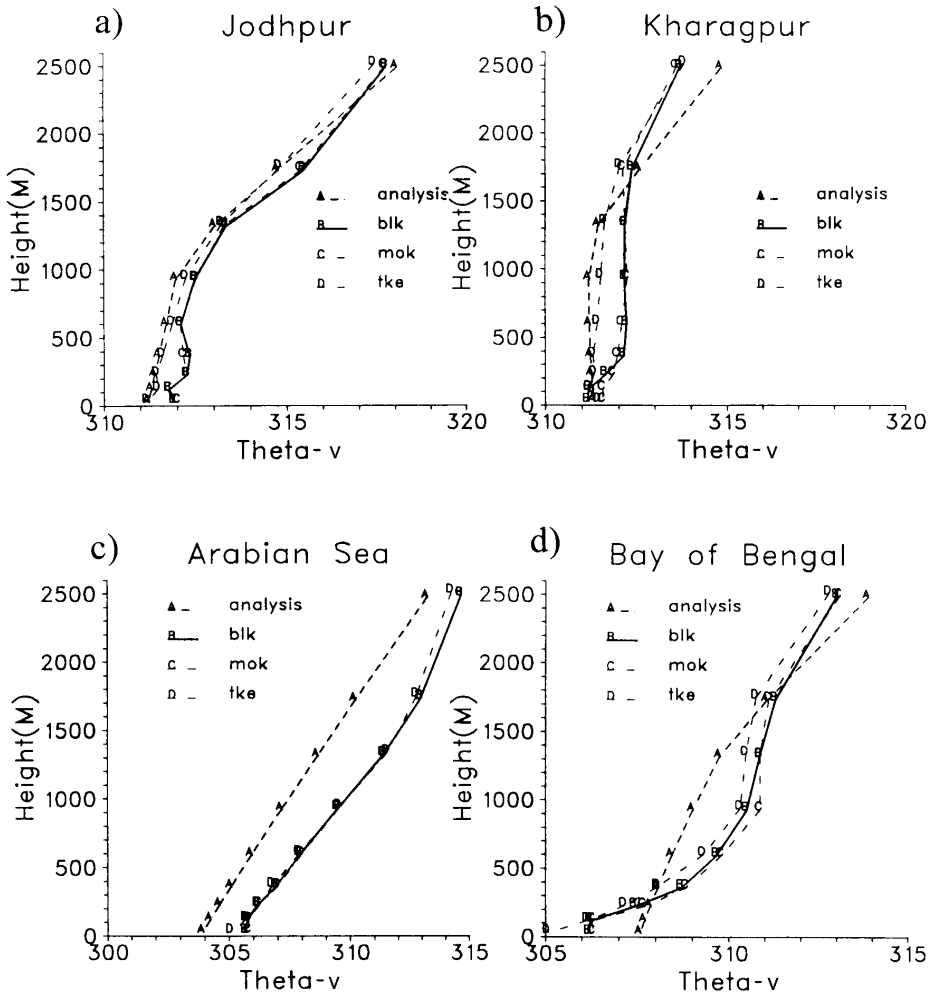

Figure 3. Vertical profiles of virtual potential temperature (θ_v) as simulated by the three boundary-layer parameterisation schemes at 1200 UTC on August 4, 1988 (24 hr forecast) and the corresponding verification analysis at (a) Jodhpur (b) Kharagpur (c) Arabian Sea and (d) Bay of Bengal.

schemes simulated similar profiles as both the experimental setups use the same method (D'Jolov, 1984) to compute K_m in the mixed layer. In the Arabian Sea and the Bay of Bengal, all the three schemes simulated similar θ_v profiles indicating that for oceanic points, results are insensitive to the type of parameterisation used.

The vertical profiles of specific humidity (g kg^{-1}) as simulated by the three parameterisation schemes are presented in Figure 4. Humidity profiles simulated by the TKE scheme are close to the verification analysis over the land points (Jodhpur and Kharagpur) as compared to the BLK and MOK schemes. Over the Arabian Sea and the Bay of Bengal, the schemes do not show much sensitivity to the type of PBL scheme used for parameterisation. The depression was located

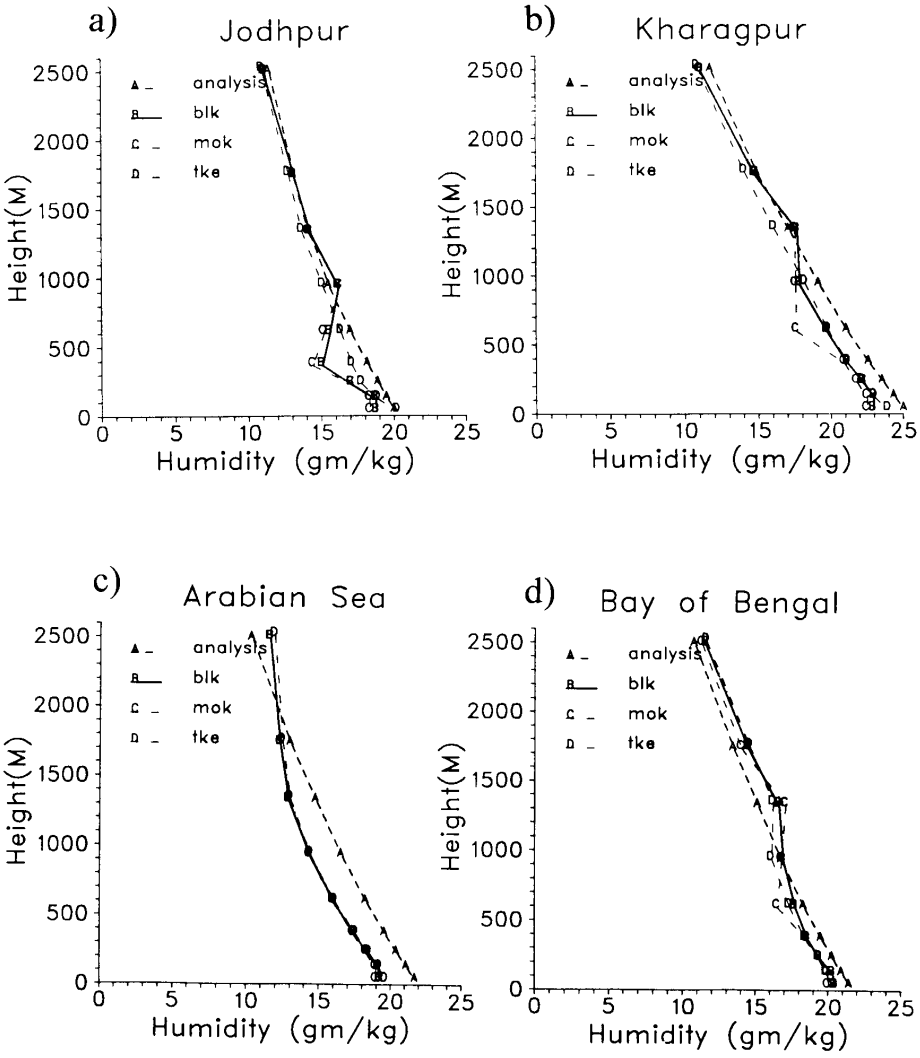

Figure 4. Same as in Figure 3 but for specific humidity.

over Jodhpur at this time. The BLK and MOK simulations departed from the observations.

Twenty-four hour simulation results of the zonal and meridional components of wind at Jodhpur, Kharagpur, Arabian Sea and Bay of Bengal are given at Figures 5 and 6 respectively. Corresponding verification analysis of 4 August 1988 at 1200 UTC is also shown. BLK, MOK and TKE simulated almost similar zonal and meridional wind profiles at sea points and at land points. Large deviation between the analysis and simulated zonal winds are noticed in the lower layers over the sea.

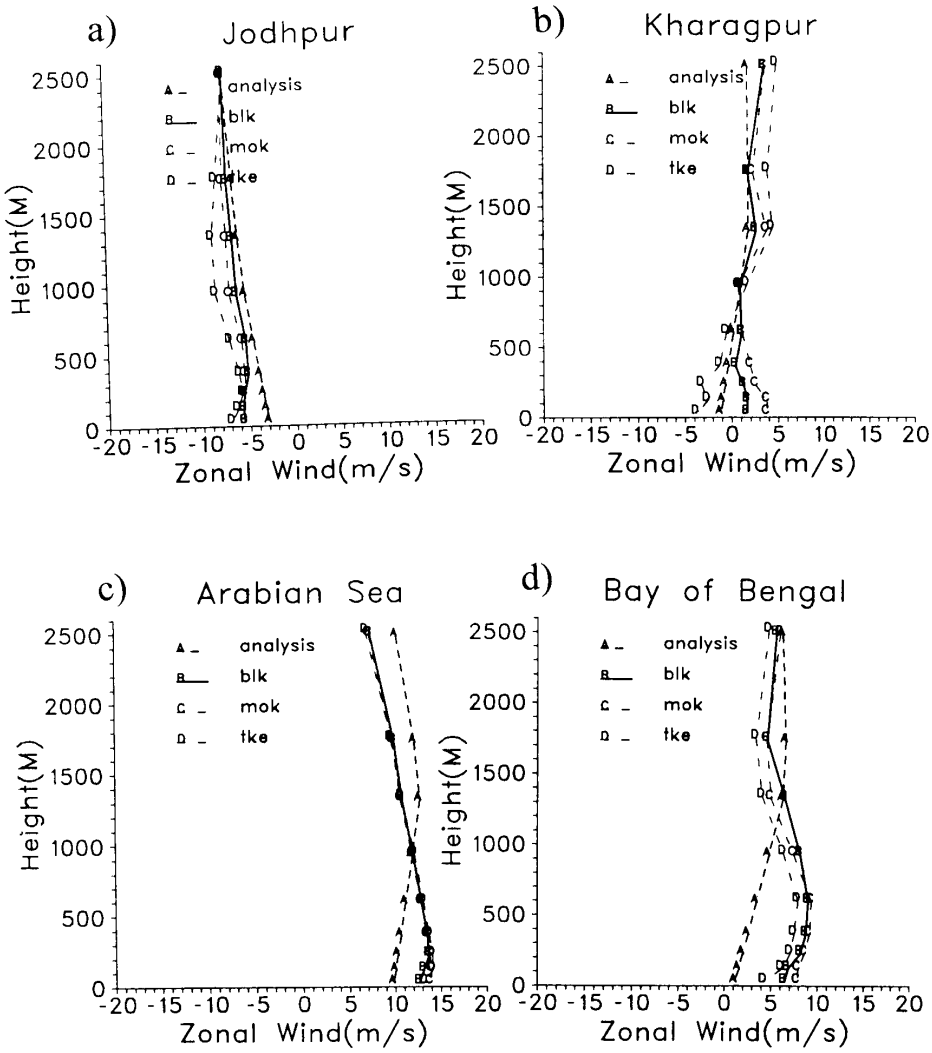

Figure 5. Same as in Figure 3 but for zonal wind.

5.2. LARGE-SCALE FIELDS

Fluxes of heat and moisture at the surface influence the temperature and humidity of the lower atmosphere as they supply heat and moisture to the different levels by means of turbulence. Figure 7 depicts the average sensible heat flux for 24 hours as simulated with the three PBL schemes (7b,c,d) at 1200 UTC, 4 August 1988 and the mean latent heat flux predicted by the bulk method (Figure 7a). Since the fluxes of latent heat predicted by all the schemes are almost similar, only that predicted by the BLK method is presented. Simulation results are in good agreement with the climatological values of latent heat flux over the Arabian Sea and the Bay of

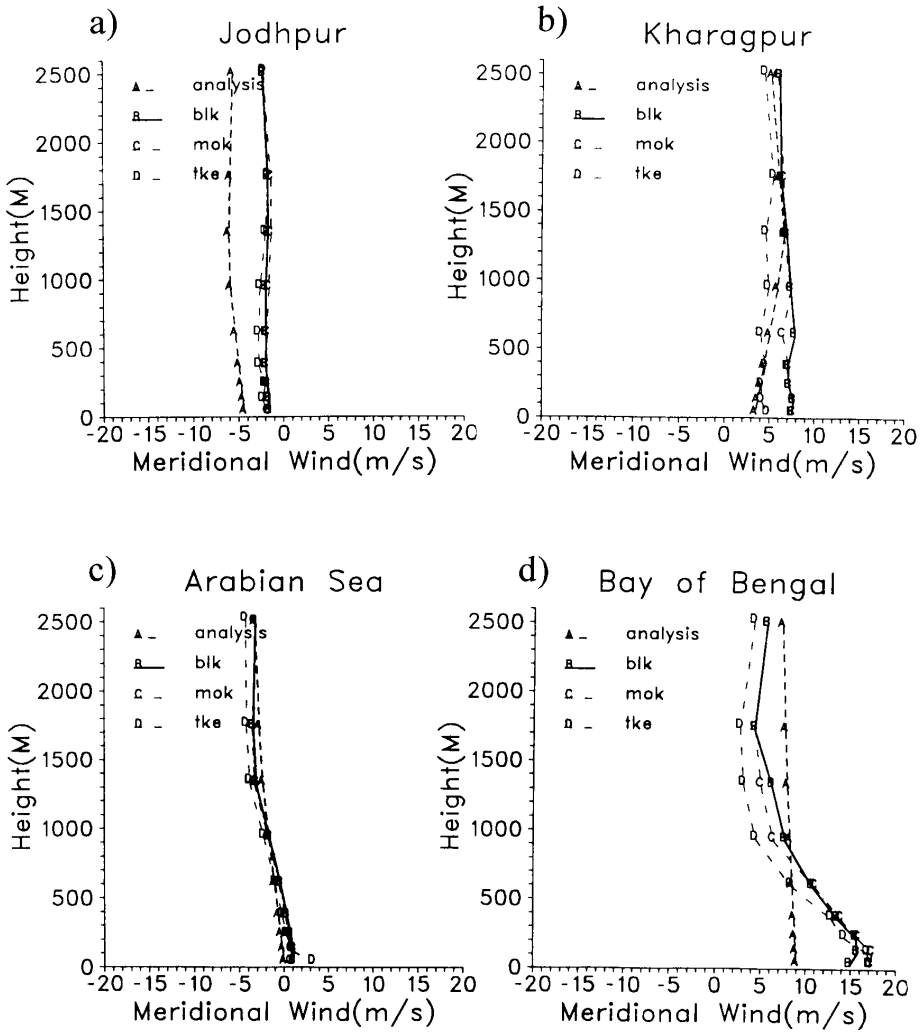

Figure 6. Same as in Figure 3 but for meridional wind.

Bengal for the month of August (Hastenrath and Lamb, 1979). In the prediction of sensible heat flux over the land region, the bulk method slightly under-predicts over the monsoon trough region. It has been observed that average sensible heat flux over the Tibetan high is about 100 Wm^{-2}. Even though the bulk method predicts sensible heat flux of 121 Wm^{-2} over the Himalayan region (Figure 7b), its magnitude is less over the trough region (67 Wm^{-2}). The first-order closure scheme predicted a high of 122 Wm^{-2} over the western end of the monsoon trough (Figure 7c) whereas TKE computed a value of 143 Wm^{-2} (Figure 7d) over the western desert region of the monsoon trough.

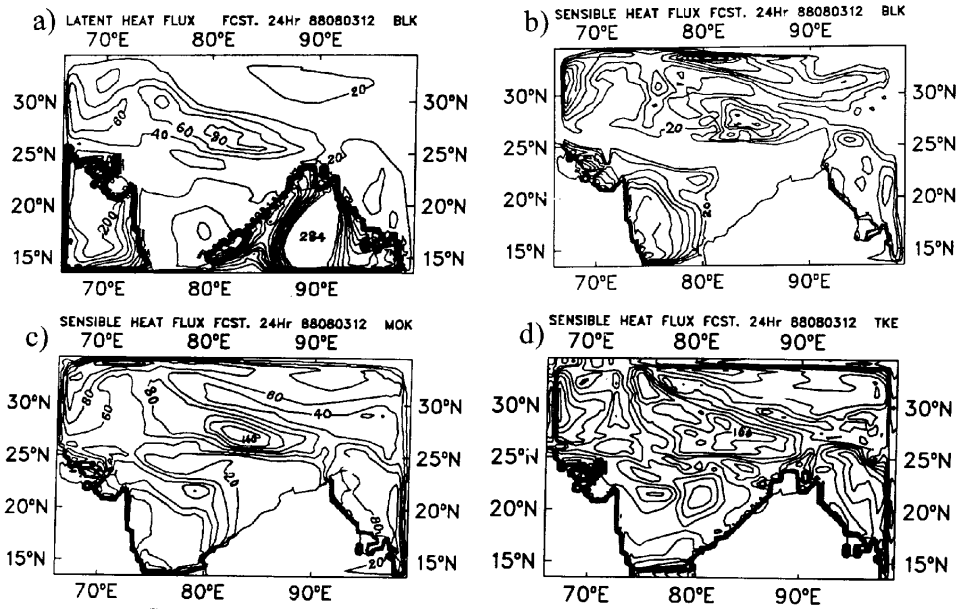

Figure 7. Model forecast (Day-1) (a) mean latent heat flux with bulk method (b) mean sensible heat flux with bulk method (c) mean sensible heat flux with first order closure scheme and (d) mean sensible heat flux with TKE scheme (units are in Wm^{-2} and contour interval is 20).

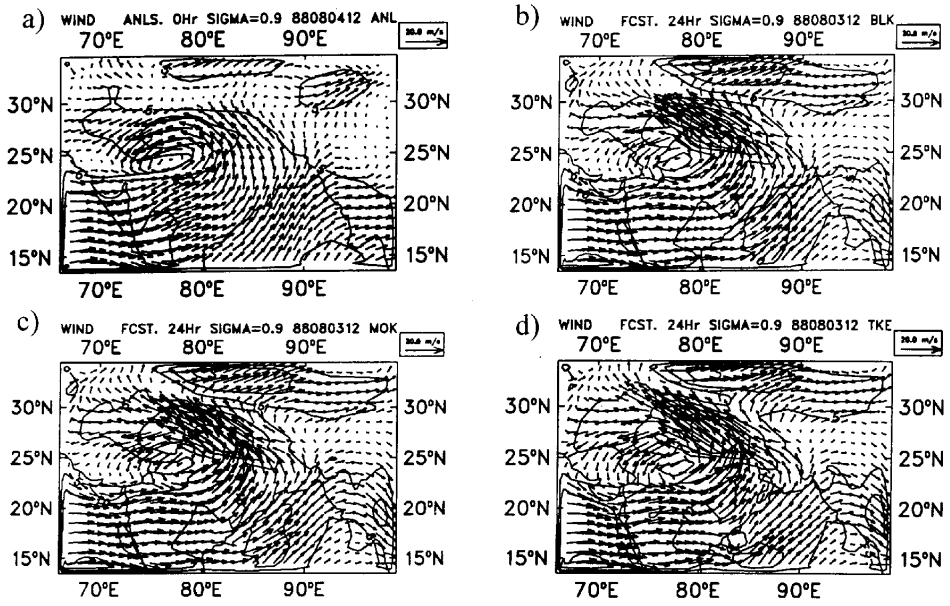

Figure 8. Analysis and model forecast (day-1) of wind vector and isotachs at the 0.9 σ level (contour interval 5 ms^{-1}) valid at 1200 UTC August 4 1988 (a) Verification analysis (b) bulk method (c) first order closure scheme and (d) TKE closure scheme.

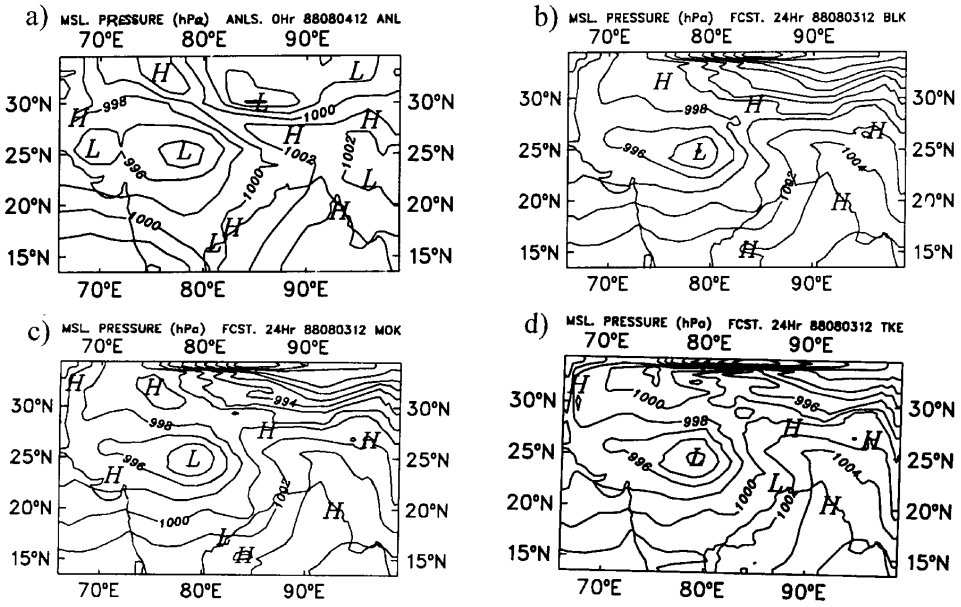

Figure 9. Same as in Figure 8 but for mean sea level pressure (contour interval: 2 hPa).

Figure 8 shows a 24 hour simulation of the wind field at the 0.9 σ level of the model and the corresponding verification analysis. Since the 0.9 σ level falls in the PBL, scrutiny of the large-scale fields at this level gives us a good idea of the impact of different parameterisation schemes. It is seen that all models have performed satisfactorily in simulating the wind fields. In all the three cases, a vortex has been developed in the simulations and the location of its centre is close to that of the verification analysis (77.3° E, 24.2° N). This feature was also apparent in the streamline fields (not shown). Magnitudes of the wind speed on the north-east side of the vortex are higher than the verification analysis. Analysed maximum wind speed in the north-east quadrant of the vortex is 12.6 m s^{-1} and that simulated by the BLK, MOK and TKE are, respectively 21.1 m s^{-1}, 22 m s^{-1} and 18 m s^{-1}. Over the Arabian Sea, wind speed and direction predicted by each PBL scheme is almost the same and agrees well with the verification analysis. Similar conclusions could be drawn from the results of a second experimental data set for 6 July 1979 at 1200 UTC (not shown).

Figure 9 depicts the mean sea level pressure simulated at 24 hours by the model with the three boundary-layer parameterisation schemes and the corresponding verifying analysis on 4 August 1988 at 1200 UTC. All the model forecasts bring out intensification of the depression and its track over 24 hours. The rate of intensification and final intensity of the system match quite well with the analysis. Pressure at the eye of the depression as given by the verification analysis was 993.1 hPa.

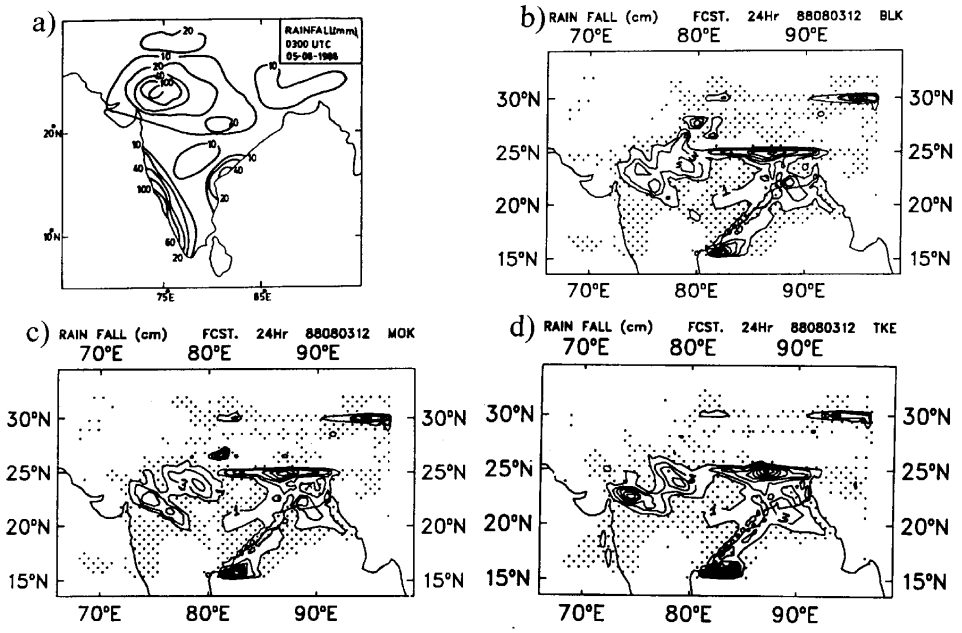

Figure 10. Rainfall for the period 03 UTC 4 August 1988 to 04 UTC 5 Aug 1988 (a) observed (source: India Meteorological Department) and as simulated by (b) bulk method (c) first-order closure scheme (d) TKE closure scheme. (Contour interval is 2 cm and the dotted area represents locations of rainfall more than 1mm but less than 1 cm).

Minimum pressures simulated at the end of 24 hours of integration by BLK, MOK and TKE were 991.9 hPa, 993.4 and 991.7 hPa respectively.

Performance of a model is also evaluated by analyzing the precipitation forecasts, an important ingredient of the NWP models. Figure 10a shows the 24 hour precipitation (observation) from 4 Aug 1988 at 0300 UTC to 5 August 1988 at 0300 UTC. Figures 11b–d show the accumulated rainfall for the same period (15 hours to 39 hours of model integration time) by models using the bulk method, first order scheme and the TKE scheme respectively. Though all the schemes were able to simulate precipitation at the east coast of India, rainfall associated with the depression is best simulated by the TKE scheme. Maximum precipitation predicted at the southern side of the depression by the BLK scheme is 68 mm per day and that by the first-order scheme is 73 mm. Maximum recorded rainfall over the region was 230 mm per day at Banswara (north-west coast of India) and the maximum precipitation predicted by TKE scheme is 163 mm per day. The TKE scheme predicted some rainfall over the Western Ghat region (22 mm) whereas the precipitation predicted by MOK and BLK models was less than 10 mm per day over the Western Ghat region during the period. Observations indicate about 30 mm per day (Figure 10a).

Table I
RMS Errors of 24 hour forecast for 1200 UTC 4 August 1988

PBL scheme	σ Level	U (m/s)	V (m/s)	T (K)	Surface pressure (hPa)
Bulk method	0.25	7.6	7.5	1.9	2.1
	0.55	2.9	2.6	1.2	
	0.9	3.3	2.5	1.8	
First order	0.25	7.7	7.5	1.9	2.1
	0.55	2.9	2.7	1.2	
	0.9	3.2	2.6	1.9	
TKE scheme	0.25	7.6	7.5	1.9	1.7
	0.55	2.9	2.7	1.2	
	0.9	3.2	2.5	1.8	

Root mean square (RMS) errors of the 24 hour forecast starting from 1200 UTC 3 August 1988 for all the three schemes are given in Table I. For surface pressure, the least RMS error is with the TKE scheme (1.7 hPa). The first-order scheme and bulk method gave identical values. At the 0.9 σ level, the least RMS error for temperature has been predicted by the bulk method as compared to the first-order and TKE schemes, though the difference between the RMS errors among the various schemes are very small. For the zonal component of wind, the least error is given by the TKE scheme (3.233 m s^{-1}). The bulk method gave the least RMS error for the meridional component of wind at the 0.9 σ level (2.490 m s^{-1}).

6. Conclusions

Numerical experiments show that, for short range forecasts, boundary-layer processes can influence the forecast of the prognostic variables substantially. Irrespective of the boundary-layer parameterisation scheme used, large-scale fields are simulated satisfactorily by all the three schemes (bulk method, first-order scheme and $1\frac{1}{2}$ order closure scheme). Specified location results show that eddy viscosity, temperature, humidity and the zonal component of wind are simulated better by the TKE scheme. For the oceanic region, the results do not show much sensitivity to the type of parameterisation scheme used. Results of heat and moisture fluxes indicate that Monin–Obukhov similarity theory is a better choice than the bulk method for the surface layer. The rms errors of mean sea level pressure and temperature are minimum for the TKE scheme. Also the TKE scheme performed better in predicting rainfall, particularly over regions of irregular terrain and over areas associated with intense synoptic systems such as the monsoon depression.

In brief, in the context of the present study, a Monin–Obukhov similarity scheme for the surface layer coupled with the TKE ($1\frac{1}{2}$ order) scheme for the mixed layer is

the best choice for the parameterisation of the PBL for simulations using a regional model over the monsoon region.

Acknowledgements

The authors would like to acknowledge the computer provided by the National Centre for Medium Range Weather Forecasting. Part of the work was supported by the Naval Research Laboratory, Washington, D.C. and by the Division of International Programs, National Science Foundation, U.S.A. Authors thank Mel DeFeo, Brenda Batts and Narender for typing the manuscript. The authors are also grateful to the anonymous referees for their very constructive and useful comments.

References

Anthes, R. A.: 1977, 'A Cumulus Parameterization Scheme Utilizing a One-Dimensional Cloud Model', *Mon. Wea. Rev.* **105**, 270–286.

Arakawa, A. and Lamb, V. R.: 1977, 'Computational Design of the Basic Dynamical Process of the UCLA General Circulation Model', in J. Chang (ed.), *Methods in Computational Physics*, Vol. 17, Academic Press, pp. 173–265.

Businger, J. A., Wyngaard, J. C., Izumi, Y., and Bradley, E. F.: 1971, 'Flux-Profile Relationships in the Atmospheric Surface Layer', *J. Atmos. Sci.* **28**, 181–189.

Charnock, H.: 1955, 'Wind Stress on a Water Surface', *Quart. J. Roy. Meteorol. Soc.* **81**, 639–640.

Clarke, R. H.: 1970, 'Recommended Methods for the Treatment of the Boundary Layer in Numerical Models of the Atmosphere', *Aust. Met. Mag.* **18**, 51–73.

D'jolov, G.D.: 1974, 'Modelling of Interdependent Diurnal Variation of Meteorological Elements in the Boundary Layer', *Khidrologiya i Meteorologiya* **23**(6), 3–20.

Daly, B. J. and Harlow, F. H.: 1970, 'Transport Equations in Turbulence', *Phys. Fluids* **13**, 2634–2649.

Deardorff, J. W.: 1972, 'Parameterisation of the Planetary Boundary Layer for Use in General Circulation Models', *Mon. Wea. Rev.* **100**, 93–106.

Deardorff, J. W.: 1974, 'Three-Dimensional Numerical Study of Turbulence in an Entraining Mixed Layer', *Boundary-Layer Meteorol.* **7**, 199–226.

Detering, H. W. and Etling, D.: 1985, 'Application of the $E-\epsilon$ Turbulence Model to the Atmospheric Boundary Layer', *Boundary-Layer Meteorol.* **33**, 113–133.

Dyer, A. J.: 1974, 'A Review of Flux-Profile Relationships', *Boundary-Layer Meteorol.* **7**, 363–372.

Hastenrath, S. and Lamb, P. J.: 1979, 'Climate Atlas of the Indian Ocean, Part I: Surface Climate and Atmospheric Circulation', University of Wisconsin Press, 112 pp.

Holt, T. and Raman, S.: 1988, 'A Review and Comparative Evaluation of Multilevel Boundary Layer Parameterisations for First-Order and Turbulent Kinetic Energy Closure Schemes', *Rev. Geophys.* **26**(4), 761–780.

Holt, T., Chang, S., and Raman, S.: 1990, 'A Numerical Study of the Coastal Cyclogenesis in GALE IOP2: Sensitivity to PBL Parameterisations', *Mon. Wea. Rev.* **118**, 234–257.

Huang, Ching-Yuang and Raman, S.: 1989, 'Application of the $E-\epsilon$ Closure Model to Simulations of Mesoscale Topographic Effects', *Boundary-Layer Meteorol.* **49**, 169–195.

Krishnamurti, T. N., Arun Kumar, K. S., Yap, A. P., Dastoor, N. D., and Sheng, J.: 1990, 'Performance of a High-Resolution Mesoscale Tropical Prediction Model', *Advances in Geophysics* **32**, 133–286.

Kumar, A.: 1989, 'A Documentation of the FSU Limited Area Model', Rep. No. 89-4, Department of Meteorology, Florida State University, Tallahassee, FL, 301 pp.

Kusuma, G. R., Raman, S., and Prabhu, A.: 1991, 'Boundary-Layer Heights over the Monsoon Trough Region During Active and Break Phases', *Boundary-Layer Meteorol.* **57**, 129–138.

Lazic, L. and Talenta, B.: 1990, 'Documentation of the UB/NMC (University of Belgrade and National Meteorological Centre, Washington) ETA model', WMO/TD No. 366.

Madala, R. V.: 1978, 'Efficient Time Integration Schemes for Atmosphere and Ocean', *Finite Difference Techniques for Vectorized Fluid Dynamics Calculations*, Springer Verlag, pp. 56–74.

Madala, R. V., Chang, S. W., Mohanty, U. C., Madan, S. C., Paliwal, R. K., Sarin, V. B., Holt, T., and Raman, S.: 1987, 'Description of Naval Research Laboratory Limited Area Dynamical Weather Prediction Model', *N.R.L. Tech. Report 5992*, Washington D.C, 131 pp.

Mahfouf, J. F., Richard, E., Mascart, P., Nickerson, E. C., and Rosset, R.: 1987, 'A Comparative Study of Various Parameterisations of the Planetary Boundary Layer in a Numerical Mesoscale Model', *J. Clim. Appl. Meteorol.* **26**, 1671–1695.

Mailhot, J. and Benoit, R.: 1982, 'A Finite Element Model of the Atmospheric Boundary Layer Suitable for use with Numerical Weather Prediction', *J. Atmos. Sci.* **39**, 2249–2266.

Mohanty, U. C., Paliwal, R. K., and Tyagi, A.: 1990, 'Application of Split-Explicit Time Integration Scheme to a Multi-level Limited Area Model and Forecast Performance over Indian Region', *Mausam* **41**, 531–540.

Monin, A. S. and Yaglom, A. M.: 1971, *Statistical Fluid Mechanics*, Vol. I, MIT Press, Cambridge, Mass., 769 pp.

Perkey, D. J. and Kreitzberg, W.: 1976, 'A Time Dependent Lateral Boundary Scheme for Limited Area Primitive Equation Models', *Mon. Wea. Rev.* **104**, 744–755.

Phillips, N. A.: 1957, 'A Coordinate System Having Some Special Advantages for Numerical Forecasting', *J. Meteorol.* **14**, 184–185.

Wyngaard, J. C.: 1975, 'Modeling the Planetary Boundary Layer-Extension to the Stable Case', *Boundary-Layer Meteorol.* **9**, 441–460.